



HAL
open science

Hepatic lentiviral gene transfer prevents the long-term onset of hepatic tumours of glycogen storage disease type 1a in mice

Julie Clar, Elodie Mutel, Blandine Gri, Alison Creneguy, Anne Stefanutti, Sophie Gaillard, Nicolas Ferry, Olivier Beuf, Gilles Mithieux, Huy Tuan Nguyen, et al.

► To cite this version:

Julie Clar, Elodie Mutel, Blandine Gri, Alison Creneguy, Anne Stefanutti, et al.. Hepatic lentiviral gene transfer prevents the long-term onset of hepatic tumours of glycogen storage disease type 1a in mice. *Human Molecular Genetics*, 2015, 24 (8), pp.2287-2296. 10.1093/hmg/ddu746 . inserm-01350897

HAL Id: inserm-01350897

<https://inserm.hal.science/inserm-01350897>

Submitted on 2 Aug 2016

HAL is a multi-disciplinary open access archive for the deposit and dissemination of scientific research documents, whether they are published or not. The documents may come from teaching and research institutions in France or abroad, or from public or private research centers.

L'archive ouverte pluridisciplinaire **HAL**, est destinée au dépôt et à la diffusion de documents scientifiques de niveau recherche, publiés ou non, émanant des établissements d'enseignement et de recherche français ou étrangers, des laboratoires publics ou privés.

**Hepatic lentiviral gene transfer prevents the long-term onset of hepatic tumours of
glycogen storage disease type 1a in mice**

Julie Clar¹⁻³, Elodie Mutel¹⁻³, Blandine Gri¹⁻³, Alison Creneguy⁵⁻⁷, Anne Stefanutti¹⁻³, Sophie Gaillard²⁻⁴, Nicolas Ferry⁷⁻⁸, Olivier Beuf²⁻⁴, Gilles Mithieux¹⁻³, Tuan Huy Nguyen⁵⁻⁷, Fabienne Rajas^{1-3*}

¹Institut National de la Santé et de la Recherche Médicale, U855, Lyon, F-69008, France

²Université de Lyon, Lyon, F-69008 France

³Université Lyon1, Villeurbanne, F-69622 France

⁴CREATIS, CNRS UMR 5220, Inserm U1044, INSA-Lyon, Villeurbanne, F-69100, France

⁵Institut National de la Santé et de la Recherche Médicale, UMRS1064, F-44093 Nantes, France

⁶CHU Hôtel Dieu, Institut de Transplantation Urologie Néphrologie, F-44093 Nantes, France

⁷Université de Nantes, F-44093 Nantes, France

⁸Institut National de la Santé et de la Recherche Médicale, UMRS948, F-44093 Nantes cedex, France

***Corresponding author:** Dr. Fabienne Rajas

Inserm U855/University Lyon 1 Laennec, 7 rue Guillaume Paradin, 69372 Lyon cedex 08
France

Tel: +33 478 77 10 28/Fax: +33 478 77 87 62

E-mail: fabienne.rajas@univ-lyon1.fr

ABSTRACT

Glycogen storage disease type 1a (GSD1a) is a rare disease due to the deficiency in the glucose-6-phosphatase catalytic subunit (encoded by *G6pc*), which is essential for endogenous glucose production. Despite strict diet control to maintain blood glucose, patients with GSD1a develop hepatomegaly, steatosis and then hepatocellular adenomas (HCA), which can undergo malignant transformation. Recently, gene therapy has attracted attention as a potential treatment for GSD1a. In order to maintain long-term transgene expression, we developed an HIV-based vector, which allowed us to specifically express the human *G6PC* cDNA in the liver. We analysed the efficiency of this lentiviral vector in the prevention of the development of the hepatic disease in an original GSD1a mouse model, which exhibits G6Pase deficiency exclusively in the liver (L-G6pc^{-/-} mice). Recombinant lentivirus were injected in B6.G6pc^{ex3lox/ex3lox}.SA^{creERT2/w} neonates and *G6pc* deletion was induced by tamoxifen treatment at weaning. Magnetic resonance imaging was then performed to follow up the development of hepatic tumours. Lentiviral gene therapy restored glucose-6 phosphatase activity sufficient to correct fasting hypoglycaemia during 9 months. Moreover, lentivirus-treated L-G6pc^{-/-} mice presented normal hepatic triglyceride levels, whereas untreated mice developed steatosis. Glycogen stores were also decreased although liver weight remained high. Interestingly, lentivirus-treated L-G6pc^{-/-} mice were protected against the development of hepatic tumours after 9 months of gene therapy while most of untreated L-G6pc^{-/-} mice developed millimetric HCA. Thus the treatment of new-borns by recombinant lentivirus appears as an attractive approach to protect the liver from the development of steatosis and hepatic tumours associated to GSD1a pathology.

Glycogen storage disease (GSD) type 1 is an inherited disease caused by the deficiency in glucose-6-phosphatase (G6Pase) activity (1–3). G6Pase catalyses the hydrolysis of glucose-6-phosphate (G6P) into glucose and inorganic phosphate, the terminal reaction in hepatic glucose production, common to glycogenolysis and gluconeogenesis. GSD type 1a (GSD1a, OMIM #232200) is caused by mutations affecting the catalytic subunit (G6PC) (4, 5) of G6Pase. G6PC is specifically expressed in the liver, kidneys and intestine, which are the only organs capable of producing glucose in the blood (6–8). Thus patients affected by GSD1a are unable to produce glucose, leading to severe hypoglycaemia during fasting in association with lactic acidemia, hypertriglyceridemia, hyperuricemia and hypercholesterolemia (2, 3, 9). Furthermore, G6Pase deficiency leads to the accumulation of G6P, glycogen and triglycerides in the liver, resulting in hepatomegaly and steatosis. The long-term complications in hepatic G6Pase deficiency include focal nodular hyperplasia and, more often, hepatocellular adenoma (HCA), with a risk of transformation into hepatocellular carcinomas (HCC) (9–11). HCAs predominantly develop during and after puberty, and more than 70% of adult GSD1 patients have multiple HCAs. In addition, patients with GSD1a also present nephropathy and intestinal disorders, which appear with time (3, 9).

The current treatment of GSD1a focuses on the prevention of hypoglycaemia and lactic acidemia through frequent meals and ingestion of uncooked cornstarch during the day, complemented by nasogastric drip-feeding of glucose or ingestion of uncooked cornstarch during the night (12). However, the underlying pathology remains uncorrected and the dietary therapy fails to prevent serious long-term complications, such as hepatic tumours. Thus tumour resection or liver transplantation are recommended if the tumours are associated with serious compression or haemorrhage, or show signs of malignant transformation into HCC

(12, 13). Recently, gene therapy has attracted attention as a potential treatment for GSD1a, since the liver is well suited for gene transfer. Indeed, the liver has been the target for *in vivo* gene therapy in many inherited metabolic diseases (14). During the last decade, several approaches of gene delivery have been evaluated in genetically engineered total *G6pc*^{-/-} mice (15) and dog colonies carrying a naturally occurring *G6pc* mutation (16). Both of these models are characterized by a very short life expectancy and death by hypoglycaemia in the absence of nutritional or gene therapy. Most studies done on these models were performed using recombinant adenovirus or adeno-associated virus (AAV). AAV-mediated therapy performed in neonates permitted a significant correction of G6Pase activity in the liver, which markedly prolonged survival, corrected hypoglycaemia during fasting and improved the biochemical parameters (see review (17, 18)). However, the hepatomegaly was only partially corrected on a long term, even if no HCA was detected in one study relating to AAV-treated total *G6pc*^{-/-} mice after 90 weeks (19). In addition, the success of AAV-based gene therapy for GSD1a is limited by a gradual loss of the transgene expression from episomal AAV vector genomes, which necessitated a re-administration of a different pseudotype of the AAV vector to sustain animals with total deficiency of G6Pase only few months after the first one (17, 20, 21). To overcome some of the limitations of AAV gene therapy, we developed a new gene delivery approach able to maintain the transgene over time, based on the use of an HIV-1-based lentiviral vector. Lentiviral vectors efficiently integrate into the host genome, providing stable long-term expression of the transgene even in cells that are actively dividing (22), and are not associated with insertional mutagenesis in the liver (23–26). The efficiency of lentiviral-mediated therapy has been validated in several animal models of inherited liver diseases, such as Crigler-Najjar type 1, Wilson disease and hemophilia (27–31).

In the present work, we studied the long-term efficacy of an HIV-based lentiviral vector carrying the human *G6PC* cDNA on the development of the hepatic disease in a new

GSD1a mouse model, which exhibits G6Pase deficiency exclusively in the liver. Interestingly, the liver-specific *G6pc* deficient (L-G6pc^{-/-}) mice show normal life expectancy and manifest all hepatic symptoms of human GSD1a pathology, including the late development of HCA (32). This allowed us to study the effect of the treatment on tumour development.

RESULTS

Correction of fasted blood glucose and hypertriglyceridemia after lentiviral gene therapy in L-G6pc^{-/-} mice

To examine the efficacy of a lentiviral gene therapy in L-G6pc^{-/-} mice, we developed an HIV-based lentiviral vector expressing the human *G6PC* cDNA under the control of a liver-specific murine transthyretin (mTTR) promoter (Fig. S1). The HIV-mTTR-hG6PC virus [4X10⁷ to 10X10⁷ transducing units] was injected in B6.G6pc^{ex3lox/ex3lox}.SA^{creERT2/w} neonates and the *G6pc* deletion was induced by tamoxifen treatment at weaning (Fig. S2). The HIV-mTTR-GFP virus [encoded GFP] was injected as control. As previously described, L-G6pc^{-/-} mice showed hypoglycaemia after 6h of fasting (Fig. 1A) (32). Indeed, blood glucose remained low in untreated L-G6pc^{-/-} mice after 6h of fasting, reaching about 50-60 mg/dL compared to 140-150 mg/dL in WT mice (Fig. 1A). On the contrary, blood glucose reached normal levels in HIV-G6PC treated L-G6pc^{-/-} mice from 2 months after *G6pc* deletion and throughout the course of the study, *i.e.* until 9 months (Fig. 1A). Concomitantly, biochemical analyses revealed that plasma TG were restored in lentivirus-treated mice (Fig. 1B). However, hypercholesterolemia was not corrected by gene therapy (Fig. 1C).

Prevention of hepatic GSD1a pathology using lentiviral gene therapy

Usually the hepatomegaly is the first symptom detected in GSD1a. It is caused by a massive G6P accumulation, leading to excessive glycogen stores. Moreover, the hepatic G6PC deficiency leads to TG accumulation in the hepatocytes, resulting in hepatic steatosis. As previously described (32), L-G6pc^{-/-} mice showed enlarged livers associated with accumulation of G6P, glycogen and TG (Fig. 2). Interestingly, hepatomegaly was partially prevented in lentivirus-treated L-G6pc^{-/-} mice (the liver accounted for 5.6±0.1% of total body mass) compared to untreated L-G6pc^{-/-} mice (the liver accounted for 9.4±0.6% of total body mass), without being normalized compared to WT mice (the liver accounted for 4.2±0.1% of total body mass) (Fig. 2A). This was associated with a substantial decrease in hepatic G6P overload (1.6±0.1 μmol G6P/g of liver in lentivirus-treated compared to 4.0±0.3 μmol G6P/g of liver in untreated L-G6pc^{-/-} mice) (Fig. 2B). Moreover, lentivirus-treated L-G6pc^{-/-} mice presented a decrease in hepatic glycogen content after 9 months of gene therapy (46.3±2.6 mg glycogen/g of liver) compared to untreated L-G6pc^{-/-} mice (69.8±4.8 mg glycogen/g of liver) (Fig. 2C). Interestingly, hepatic steatosis was substantially prevented by lentiviral gene therapy since hepatic TG content of lentivirus-treated L-G6pc^{-/-} mice was lower than that of untreated L-G6pc^{-/-} mice and not significantly different as that of the WT mice (Fig. 2D). Histological observations of the livers of untreated L-G6pc^{-/-} mice confirmed a marked steatosis, with an enlargement of hepatocytes containing large lipid vacuoles, mainly in the periportal areas (Fig. 3A, panel b). Lentivirus-treated L-G6pc^{-/-} mice exhibited large areas showing normal appearance of hepatocytes. However, some areas with enlarged hepatocytes were still observed (Fig. 3A, panel c). Moreover, serial section analyses performed in the liver of lentivirus-treated L-G6pc^{-/-} mice revealed that hepatocytes expressing G6PC, detected by immunohistochemistry (Fig. 3B panels b), presented a normal morphology with an absence of lipid vacuoles (Fig. 3B, panels a). On the contrary, the areas with steatosis matched perfectly

with $G6pc^{-/-}$ hepatocytes, which did not express G6PC (Fig. 3B). To confirm that hepatocytes expressing G6PC were corrected cells, we analysed the expression of human $G6pc$ mRNA in the lentivirus-treated liver compared to that of the mouse $G6pc$ mRNA of WT liver. As expected, the human $G6pc$ mRNA was undetectable in untreated mice and was substantially expressed in lentivirus-treated mice. Quantitatively, its expression was 10 fold lower than that of endogenous mouse $G6pc$ mRNA in the WT liver (Fig. 3C). It may be noted that the transcription of a truncated mouse $G6pc$ mRNA (containing exon 1 and 2) was up regulated in L- $G6pc^{-/-}$ liver, as previously reported (32). Consistent with a decrease in glycogen stores and normalization of hepatic TG levels, none of the HIV-G6PC treated L- $G6pc^{-/-}$ mice (total of 11) developed hepatic tumours, as observed by MRI analysis after 9 months of gene therapy. On the contrary, most untreated L- $G6pc^{-/-}$ mice (17 out of 24) had multiple millimetric hepatic lesions (1 to 4 mm of diameter) at the end of the experiment (Fig. 4A-B). Almost all lesions corresponded to HCA (Fig. 4C and E), with the exception of one found in an untreated L- $G6pc^{-/-}$ mouse, which developed an HCC (Fig. 4D and F).

Mosaic restoration of G6PC in L- $G6pc^{-/-}$ livers after gene therapy

As previously observed, G6Pase was mainly expressed in the periportal area compared to the perivenous area of the liver in the WT mice (Fig. 5A, panels a-b). In agreement with the deletion of $G6pc$, G6PC protein was undetectable by immunohistochemistry in untreated L- $G6pc^{-/-}$ mice (Fig. 5A panels c-d). Interestingly, G6PC was specifically localized in hepatocytes found in the close vicinity of blood vessels after 6 weeks post-injection in lentivirus-treated L- $G6pc^{-/-}$ mice; these hepatocytes exhibited high immunostaining for G6PC whereas a substantial proportion of the surrounding hepatocytes were G6PC-negative (Fig. 5A panels e-f). After 9 months of gene therapy, lentivirus-treated L- $G6pc^{-/-}$ hepatocytes presented a patchy localization of the G6PC protein, in both the periportal and perivenous areas (Fig. 5A panels g-h). Thus immunostaining of G6PC was observed in large and diffuse

areas around vessels. The presence of large and diffuse G6PC positive areas around vessels 9 months after the lentiviral gene therapy was probably due to hepatocyte divisions. Indeed, lentivirus-treated L-G6pc^{-/-} mice exhibited an increased number in transduced hepatocytes, from $8 \pm 3.5\%$ at 6 weeks to 18 ± 0.9 at 9 months after hepatocyte transduction (Fig. 5B). Moreover, the G6Pase activity in the liver represented about 25% of WT hepatic G6Pase activity at 9 months post-injection, respectively (Fig. 5C). Finally, it is noteworthy that the DNA transgene was detected in several tissues after lentiviral gene therapy because the viral vectors were injected into the bloodstream (Fig. 5D). Nine months after gene therapy, the viral vector copy numbers were determined in the livers of lentivirus-treated mice by qPCR and found to represent about 3 copies per 100 cells. As expected, the human *G6PC* transgene was mainly expressed in the liver, although we observed a small leak in the spleen (data not shown).

DISCUSSION

Since the 1980s, dietary management to achieve suitable metabolic control has considerably improved the life expectancy of GSD1 patients, but various complications occur with aging. One of the main causes of morbidity and mortality in aging GSD1 patients derives from the development of HCA. Most patients develop many HCAs, which can grow, become haemorrhagic or malignant over time (10–12). In this context, liver gene therapy provides an attractive alternative to liver transplantation, which is currently the only effective therapy performed on the basis of serious impairment of metabolic control or risk of malignant transformation. To date, the most promising gene therapy approaches to treat GSD1a were focused on the use of AAV in order to achieve efficient *in vivo* gene transfer in the liver (17, 18). However, AAV vectors rarely integrate into the host genome, remaining primarily in an

episomal form, and thus providing prolonged transgene expression only in the absence of cell division (33). Even after delivery in adult mice, a gradual loss of the transgene expression and of the therapeutic effect may be expected because of the turnover (even low) of hepatocytes (34, 35). In addition, because of some cross-reactivity of neutralizing antibodies across AAV serotypes, the re-injection of a second AAV different from the first one may be inefficient. In contrast to AAVs, lentiviral vectors efficiently integrate into the cellular genome, providing long-term expression, in both quiescent cells and cells that are actively dividing (24). However, it appeared that lentiviral vectors transduce less efficiently the cells that are in the G0 state of the cell cycle, such as differentiated adult hepatocytes (14, 24, 36). Moreover, an immune response to the therapeutic protein could also preclude the long-term correction of the disease (24). New strategies have been devised to prevent the expression of the transgene in antigen-presenting cells and thus to bypass the immune response (24). It must be mentioned that a previous study using a feline lentivirus expressing the human *G6PC* cDNA was performed at a neonatal stage, to avoid an immune response against the transgene components (37). This allowed the authors to normalize blood glucose and to attenuate the hepatic disease (i.e. a decrease in glycogen accumulation) in the total knockdown *G6pc* mouse after a double neonatal virus administration. Here we report the use of a similar recombinant vector, i.e. an HIV-based lentiviral vector carrying the human *G6PC* cDNA under the liver-specific mTTR promoter. It is noteworthy that this study was performed in L.*G6pc*^{-/-} mice exhibiting a long life expectancy that allowed us to study the effect of the lentiviral treatment on tumour development, a question not addressed in the former study. Interestingly, the HCA development seems to be accelerated in mice treated with tamoxifen at the age of 3 weeks, compared with mice treated at adult age (6-8 weeks). Indeed, small hepatic nodules of about 3-4 mm in diameter were detected in most untreated L.*G6pc*^{-/-} mice after 9 months of *G6pc* deletion, whereas only 20-30% L.*G6pc*^{-/-} mice showed millimetric

nodules when *G6pc* deletion was performed in adults (32). In our study, lentiviral gene therapy restored about 25% of basal hepatic G6Pase activity that enabled the treated L-*G6pc*^{-/-} mice to maintain normal fasting blood glucose levels and to normalize hypertriglyceridemia for 9 months. Moreover, lentivirus-treated L-*G6pc*^{-/-} mice presented a decrease in hepatic glycogen stores and a normalization of TG contents, at 9 months after gene therapy. In addition, lentivirus-treated mice did not show hepatic lesions after 9 months while most of untreated L-*G6pc*^{-/-} mice developed HCA at this time. It is noteworthy that a recent study reported the prevention of HCA in the total *G6pc* KO mice treated by an AAV approach, despite hepatomegaly and elevated hepatic glycogen stores (19). However, the AAV-treated *G6pc* KO mice exhibited no steatosis and had normal levels of hepatic TG (19). Taken together with the study here, these data suggest that the excessive lipid accumulation rather than the glycogen accumulation could be the cause of the long-term consequence of HCA developed in L-*G6pc*^{-/-} mice. Interestingly, many evidence suggest that nonalcoholic fatty liver disease, which is characterized by hepatic steatosis, is associated with the development of hepatic tumours, without overt hepatic fibrosis or cirrhosis (38, 39). Some hypothetical mechanisms include oxidative stress, adipocytokine functional disorder, or chronic inflammation linked to lipotoxicity (40). Further studies should be conducted to highlight the central role of fatty liver in tumour development. In our study, the prevention of HCA formation with lentiviral gene therapy is associated with the presence of large and diffuse areas expressing G6PC, representing about 20% of the liver surface (see Fig. 5A panels g-h and 5B). This is probably due to the transgene integration into the host genome and transmission during hepatocyte divisions in the neonatal liver. The clonal expansion of transduced cells could be explained by a selective advantage to treated cells. However, long-term studies will be required to know whether the liver GSD1a disease is only improved for a while or whether it is cured definitely. Indeed, the rescue of a partial G6Pase activity in a low

proportion of hepatocytes could only permit to maintain blood glucose level and will not cure the rest of hepatocytes, which will still be prone to hepatic tumour development with time. Contrarily to monogenic diseases that involve a primary defect in a hepatic protein without significant parenchymal damage and hepatic injury, such as Crigler-Najjar disease or coagulation defects, gene therapy approach of GSD1a has to correct a maximum of *G6pc*^{-/-} hepatocytes in order to prevent at best the development of the hepatic disease. Contrarily, Crigler-Najjar disease or coagulation defects only require the expression of only low levels of the related hepatic protein in the blood stream to treat or prevent the systemic illness manifestations.

Finally, in comparison to gamma retroviral LTR-driven vectors, lentiviral vectors present with favourable features like a potentially safer insertion profile. Thus our study supports the absence of genotoxicity of HIV1-derived lentiviral vectors in the liver (23, 25). However, the residual genotoxicity risk associated with the preferential intragenic integration events represents the most obvious concern. The substantial flexibility of the lentiviral vector genome offers opportunities for redesigning sequences of the backbone as well as the therapeutic cargo to further reduce this risk.

In conclusion, we demonstrate here that the lentiviral gene therapy performed during the neonate period permits a strong expression of G6Pase, corrects fasting blood glucose levels and prevents the hepatic disease, including the HCA formation, for at least 9 months in L-*G6pc*^{-/-} mice. However, more efficient approaches are still needed to improve all parameters, including glycogen stores. A specific and stronger hepatic expression of the transgene could be obtained by adding regulatory sequences to the mTTR promoter (30, 41, 42). Moreover, since the mTTR promoter is leaky permitting a weak expression in non-liver cells, in particular in antigen presenting cells, the addition of mir142-3pT sequence in the vector backbone would be useful to prevent an immune rejection of transduced cells (27, 43). In

addition, it is interesting to note that the lentiviral vector gene therapy permits the transduction of the three organs affected by GSD1a, i.e. the liver, kidney and intestine (see Fig.5D). This indicates that this approach might be suitable as a possible treatment of the kidney or intestine diseases if combined with the use of an appropriate promoter. Because a neonatal intervention in a clinical setting may drastically improve the phenotype in the most critical years of an infant development, the lentiviral gene therapy appears as an attractive approach for GSD1a treatment.

MATERIALS AND METHODS

Preparation of recombinant vectors encoding human G6PC

We produced an HIV-based lentiviral vector carrying the human G6PC cDNA (or the GFP cDNA as control) under the control of the murine transthyretin (mTTR) promoter, fused to a synthetic hepatocyte-specific enhancer that specifically directs transcription to the liver (28), that specifically directs transcription to the liver. High-titre lentiviral vector stocks were generated as previously described by calcium phosphate-mediated transient transfection of three plasmids: the transfer vector plasmid, the packaging plasmid psPAX2, and the vesicular stomatitis virus G protein (VSV G) envelope protein-coding plasmid pMD2G (44). These self-inactivating transfer vectors harboured the *cis*-acting cPPT/CTS from HIV-1, which facilitates the nuclear translocation of preintegrative vector complexes (45, 46) and the posttranscriptional regulatory element from the woodchuck hepatitis virus, which increase transgene expression (47) and was inserted downstream of the transgene (Fig. S1). The titres of the viral preparations were determined as previously described (28) and were in the range of $1-2 \times 10^9$ transducing units/mL.

AAV and lentiviral vector administration into mice

Two-day old B6.G6pc^{ex3lox/ex3lox}.SA^{creERT2/w} mice were infused *via* the temporal vein with 50 μ L of HIV-mTTR-hG6PC virus (n= 11) or HIV-mTTR-hGFP virus containing 4×10^7 to 10×10^7 transducing units in phosphate-buffered saline. Mice of the untreated group (n=24) corresponded to HIV-mTTR-hGFP injected mice.

Generation of liver-specific G6pc knock-out mice

The deficiency in G6Pase was obtained by a specific deletion of *G6pc* exon 3 in the liver, using a CRE-lox strategy (32). B6.G6pc^{ex3lox/ex3lox}.SA^{creERT2/w} and C57Bl/6J mice (Charles Rivers Laboratories, L'Arbresle, France) of both genders were injected intraperitoneally at 15-21 day old with 0.5 mg of tamoxifen every day for four consecutive days, in order to obtain L-G6pc^{-/-} and wild-type (WT) mice, respectively. Mice were housed in the animal facility of Lyon 1 University under temperature controlled (22°C) conditions and with a 12/12 h light/dark cycle. Mice had free access to water and standard chow diet. Fasted mice were provided with continuous access to water. All the procedures were performed in accordance with the principles and guidelines established by the European Convention for the Protection of Laboratory Animals. The animal care committee of University Lyon 1 approved all the experiments.

Magnetic resonance imaging

Magnetic resonance imaging (MRI) examinations were performed 5, 7 and 9 months after *G6pc* deletion on anesthetized mice on an horizontal 4.7T Biospec system (Bruker, Ettlingen, Germany) (32). T2-weighted contrast images were acquired in the axial plane with a fat suppressed rapid acquisition with relaxation enhanced (RARE) sequence with the following parameters: repetition time > 6 sec; 38.2 ms echo time; 30 x 30 mm² Field of View, 256 x 192 matrix, 32 slices of 0.7 mm thick; RARE factor = 4; 2 averages; 98 Hz of pixel bandwidth. A

trained radiologist who has over twenty years of experience analysed the MR images to detect nodules *in vivo*.

Biochemical assays

Blood glucose was followed after 6 h of fasting with an Accu-Chek Go glucometer (Roche Diagnostics, Meylan, France). Blood was withdrawn by submandibular bleeding using a lancet and collected into EDTA. Plasma triglycerides and cholesterol were determined with Biomérieux colorimetric kits (Marcy l'Etoile, France). Mice were killed by cervical dislocation. The liver was immediately removed, weighed and snap-frozen using tongs previously chilled in liquid N₂ and stored at -80°C. All tissues were analysed macroscopically. Hepatic glycogen determinations were carried out on frozen tissue homogenates according to the procedure previously described (48). Total hepatic lipids were extracted by the method of Bligh and Dyer (49), and triglyceride content was measured using a Biomérieux colorimetric kit. Hepatic G6Pase activity was assayed at maximal velocity (20 mmol/l of G6P) at 30°C, as previously described (50).

Gene expression

Total RNAs were extracted from livers with TRIzol reagent (InVitrogen life technology, St Aubin, France), according to the manufacturer's instructions. Reverse transcription was performed using the kit QuantiTect Reverse transcription (Quiagen France, Courtabeuf). Quantitative PCR was performed using the Advanced Universal SYBR Green Supermix (Bio-Rad Laboratories, Marnes-la-Coquette) in the CFX Manager Realplex (Bio-Rad). Endogenous *G6pc* exon 1-exon 3 mRNA fragment was amplified using exon 1 *mG6pc* sense 5'TTACCAAGACTCCCAGGACTG3' and exon 2 *mG6pc* antisense 5'GAGCTGTTGCTGTAGTAGTCG3'. The specific human *G6PC* exon 4-exon 5 mRNA fragment was amplified using exon 2 *mG6pc* sense 5'AGCGTCCATACTGGTGGGTTT3'

and exon 3 *mG6pc* antisense 5'GGTCGGCTTTATCTTTCCCTG3'. The mouse ribosomal protein L19 transcript (Rpl19) was used as housekeeping gene (32). Calculations were based on the comparative cycle threshold method ($2^{-\Delta\Delta Ct}$).

Histological analysis

A piece of the liver and hepatic nodules were fixed in 10% formalin for histological analyses and embedded in paraffin. Serial sections (4 μ m thick) were cut and stained with hematoxylin and eosin (H&E) staining. Immunohistochemical analyses were performed as previously described, using a purified rabbit anti-G6PC antibody (dilution 1:1,000) (51). The slides were examined under a Coolscope microscope (Nikon Instruments, New York, US). The G6PC-positive cell index was calculated and expressed as the percentage of positive stained area against total analysed area.

The following criteria were used to identify HCA and HCC. HCA were defined as nodules, visible at macroscopic examination, well circumscribed, expansive, compressing the adjacent parenchyma. They were made of well-differentiated hepatocytes, usually larger than normal hepatocytes, with low nuclear-cytoplasmic ratio, eosinophilic, clear or vacuolated cytoplasm, and enlarged nuclei with well visible nucleoli. The normal trabecular architecture was retained; plates were regular and 1 to 2 cells thick. No connective septa were present. Mitotic figures were rare. In some cases, smaller basophilic, proliferative hepatocytes could be observed, usually at the periphery of the nodule; cell atypia might be present but only focally; no evidence of local tissue invasion or angioinvasion was detected. HCC was defined by the presence of architectural and cellular atypia. The architecture was mainly trabecular but plates were irregular, usually 2 to 4-cell thick branched and separated by dilated and capillarized sinusoidal vessels. Hepatocytes were of variable size, but were frequently characterized by low nuclear-cytoplasmic ratio and basophilic cytoplasm. Nuclear atypia was frequent. Mitoses

were numerous. Connective septa could be present. Tissue invasion and/or angioinvasion might be detected.

ACKNOWLEDGMENTS

This work was supported by research grants from the “Agence Nationale de la Recherche” [ANR-07-MRAR-011-01, ANR11-BSV1-009-01]; the “Association Française contre les Myopathies”; and the “Association Francophone des Glycogénoses”.

Authors would like to thank the members of the animal facility of Lyon 1 University (ALECS, SFR Santé Lyon-Est, Lyon), the members of the CECIL platform (Université Lyon 1 Laennec), the Vector Core facility of the University Hospital of Nantes-INSERM UMR 1089 for providing the AAV vectors, and the members of the Anipath Platform (headed by Pr. Jean-Yves Scoazec; Université Lyon 1 Laennec). We also thank Pr. Frank Pilleul (Lyon) for the reading of the MRI images and Pr. Jean-Yves Scoazec for his histological description of HCA and HCC in mice (see Material & Methods).

Conflict of interest statement: The authors who have taken part in this study declare that they do not have anything to disclose regarding funding or there is no conflict of interest with respect to this manuscript.

REFERENCES

1. Shelly, L.L., Lei, K.J., Pan, C.J., Sakata, S.F., Ruppert, S., Schutz, G. and Chou, J.Y. (1993) Isolation of the gene for murine glucose-6-phosphatase, the enzyme deficient in glycogen storage disease type 1A. *J. Biol. Chem.*, **268**, 21482–21485.
2. Chou, J.Y., Matern, D., Mansfield, B.C. and Chen, Y.-T. (2002) Type I glycogen storage diseases: disorders of the glucose-6-phosphatase complex. *Curr. Mol. Med.*, **2**, 121–143.
3. Froissart, R., Piraud, M., Boudjemline, A.M., Vianey-Saban, C., Petit, F., Hubert-Buron, A., Eberschweiler, P.T., Gajdos, V. and Labrune, P. (2011) Glucose-6-phosphatase deficiency. *Orphanet J. Rare Dis.*, **6**, 27.
4. Bruni, N., Rajas, F., Montano, S., Chevalier-Porst, F., Maire, I. and Mithieux, G. (1999) Enzymatic characterization of four new mutations in the glucose-6 phosphatase (G6PC) gene which cause glycogen storage disease type 1a. *Ann. Hum. Genet.*, **63**, 141–146.
5. Lei, K.J., Shelly, L.L., Pan, C.J., Sidbury, J.B. and Chou, J.Y. (1993) Mutations in the glucose-6-phosphatase gene that cause glycogen storage disease type 1a. *Science*, **262**, 580–583.
6. Mithieux, G., Rajas, F. and Gautier-Stein, A. (2004) A novel role for glucose 6-phosphatase in the small intestine in the control of glucose homeostasis. *J. Biol. Chem.*, **279**, 44231–44234.
7. Mithieux, G., Bady, I., Gautier, A., Croset, M., Rajas, F. and Zitoun, C. (2004) Induction of control genes in intestinal gluconeogenesis is sequential during fasting and maximal in diabetes. *Am. J. Physiol. Endocrinol. Metab.*, **286**, E370–375.

8. Rajas, F., Bruni, N., Montano, S., Zitoun, C. and Mithieux, G. (1999) The glucose-6 phosphatase gene is expressed in human and rat small intestine: regulation of expression in fasted and diabetic rats. *Gastroenterology*, **117**, 132–139.
9. Rake, J.P., Visser, G., Labrune, P., Leonard, J.V., Ullrich, K. and Smit, G.P.A. (2002) Glycogen storage disease type I: diagnosis, management, clinical course and outcome. Results of the European Study on Glycogen Storage Disease Type I (ESGSD I). *Eur. J. Pediatr.*, **161 Suppl 1**, S20–34.
10. Calderaro, J., Labrune, P., Morcrette, G., Rebouissou, S., Franco, D., Prévot, S., Quaglia, A., Bedossa, P., Libbrecht, L., Terracciano, L., *et al.* (2013) Molecular characterization of hepatocellular adenomas developed in patients with glycogen storage disease type I. *J. Hepatol.*, **58**, 350–357.
11. Franco, L.M., Krishnamurthy, V., Bali, D., Weinstein, D.A., Arn, P., Clary, B., Boney, A., Sullivan, J., Frush, D.P., Chen, Y.-T., *et al.* (2005) Hepatocellular carcinoma in glycogen storage disease type Ia: a case series. *J. Inherit. Metab. Dis.*, **28**, 153–162.
12. Rake, J.P., Visser, G., Labrune, P., Leonard, J.V., Ullrich, K. and Smit, G.P.A. (2002) Guidelines for management of glycogen storage disease type I - European Study on Glycogen Storage Disease Type I (ESGSD I). *Eur. J. Pediatr.*, **161 Suppl 1**, S112–119.
13. Faggioli, S., Daina, E., D'Antiga, L., Colledan, M. and Remuzzi, G. (2013) Monogenic diseases that can be cured by liver transplantation. *J. Hepatol.*, **59**, 595–612.
14. Nguyen, T.H. and Ferry, N. (2004) Liver gene therapy: advances and hurdles. *Gene Ther.*, **11 Suppl 1**, S76–84.
15. Lei, K.J., Chen, H., Pan, C.J., Ward, J.M., Mosinger, B. Jr, Lee, E.J., Westphal, H., Mansfield, B.C. and Chou, J.Y. (1996) Glucose-6-phosphatase dependent substrate transport

in the glycogen storage disease type-1a mouse. *Nat. Genet.*, **13**, 203–209.

16. Kishnani, P.S., Faulkner, E., VanCamp, S., Jackson, M., Brown, T., Boney, A., Koeberl, D. and Chen, Y.T. (2001) Canine model and genomic structural organization of glycogen storage disease type Ia (GSD Ia). *Vet. Pathol.*, **38**, 83–91.

17. Koeberl, D.D. (2012) In search of proof-of-concept: gene therapy for glycogen storage disease type Ia. *J. Inherit. Metab. Dis.*, **35**, 671–678.

18. Chou, J.Y. and Mansfield, B.C. (2011) Recombinant AAV-directed gene therapy for type I glycogen storage diseases. *Expert Opin. Biol. Ther.*, **11**, 1011–1024.

19. Lee, Y.M., Jun, H.S., Pan, C.-J., Lin, S.R., Wilson, L.H., Mansfield, B.C. and Chou, J.Y. (2012) Prevention of hepatocellular adenoma and correction of metabolic abnormalities in murine glycogen storage disease type Ia by gene therapy. *Hepatol. Baltim. Md*, **56**, 1719–1729.

20. Demaster, A., Luo, X., Curtis, S., Williams, K.D., Landau, D.J., Drake, E.J., Kozink, D.M., Bird, A., Crane, B., Sun, F., *et al.* (2012) Long-term efficacy following readministration of an adeno-associated virus vector in dogs with glycogen storage disease type Ia. *Hum. Gene Ther.*, **23**, 407–418.

21. Ghosh, A., Allamarvdasht, M., Pan, C.J., Sun, M.S., Mansfield, B.C., Byrne, B.J. and Chou, J.Y. (2006) Long-term correction of murine glycogen storage disease type Ia by recombinant adeno-associated virus-1-mediated gene transfer. *Gene Ther.*, **13**, 321–329.

22. Zahler, M.H., Irani, A., Malhi, H., Reutens, A.T., Albanese, C., Bouzahzah, B., Joyce, D., Gupta, S. and Pestell, R.G. (2000) The application of a lentiviral vector for gene transfer in fetal human hepatocytes. *J. Gene Med.*, **2**, 186–193.

23. Rittelmeyer, I., Rothe, M., Brugman, M.H., Iken, M., Schambach, A., Manns, M.P., Baum, C., Modlich, U. and Ott, M. (2013) Hepatic lentiviral gene transfer is associated with clonal selection, but not with tumor formation in serially transplanted rodents. *Hepatology*, **58**, 397–408.
24. Ferry, N., Pichard, V., Sébastien Bony, D.A. and Nguyen, T.H. (2011) Retroviral vector-mediated gene therapy for metabolic diseases: an update. *Curr. Pharm. Des.*, **17**, 2516–2527.
25. Themis, M., Waddington, S.N., Schmidt, M., von Kalle, C., Wang, Y., Al-Allaf, F., Gregory, L.G., Nivsarkar, M., Themis, M., Holder, M.V., *et al.* (2005) Oncogenesis following delivery of a nonprimate lentiviral gene therapy vector to fetal and neonatal mice. *Mol. Ther. J. Am. Soc. Gene Ther.*, **12**, 763–771.
26. Schambach, A., Zychlinski, D., Ehrnstroem, B. and Baum, C. (2013) Biosafety features of lentiviral vectors. *Hum. Gene Ther.*, **24**, 132–142.
27. Schmitt, F., Remy, S., Dariel, A., Flageul, M., Pichard, V., Boni, S., Usal, C., Myara, A., Laplanche, S., Anegon, I., *et al.* (2010) Lentiviral vectors that express UGT1A1 in liver and contain miR-142 target sequences normalize hyperbilirubinemia in Gunn rats. *Gastroenterology*, **139**, 999–1007, 1007.e1–2.
28. Nguyen, T.H., Bellodi-Privato, M., Aubert, D., Pichard, V., Myara, A., Trono, D. and Ferry, N. (2005) Therapeutic lentivirus-mediated neonatal in vivo gene therapy in hyperbilirubinemic Gunn rats. *Mol. Ther. J. Am. Soc. Gene Ther.*, **12**, 852–859.
29. Merle, U., Encke, J., Tuma, S., Volkmann, M., Naldini, L. and Stremmel, W. (2006) Lentiviral gene transfer ameliorates disease progression in Long-Evans cinnamon rats: an animal model for Wilson disease. *Scand. J. Gastroenterol.*, **41**, 974–982.
30. Brown, B.D., Cantore, A., Annoni, A., Sergi, L.S., Lombardo, A., Della Valle, P.,

D'Angelo, A. and Naldini, L. (2007) A microRNA-regulated lentiviral vector mediates stable correction of hemophilia B mice. *Blood*, **110**, 4144–4152.

31. Matsui, H., Hegadorn, C., Ozelo, M., Burnett, E., Tuttle, A., Labelle, A., McCray, P.B., Naldini, L., Brown, B., Hough, C., *et al.* (2011) A microRNA-regulated and GP64-pseudotyped lentiviral vector mediates stable expression of FVIII in a murine model of Hemophilia A. *Mol. Ther. J. Am. Soc. Gene Ther.*, **19**, 723–730.

32. Mutel, E., Abdul-Wahed, A., Ramamonjisoa, N., Stefanutti, A., Houberdon, I., Cavassila, S., Pilleul, F., Beuf, O., Gautier-Stein, A., Penhoat, A., *et al.* (2011) Targeted deletion of liver glucose-6 phosphatase mimics glycogen storage disease type 1a including development of multiple adenomas. *J. Hepatol.*, **54**, 529–537.

33. Alexander, I.E., Cunningham, S.C., Logan, G.J. and Christodoulou, J. (2008) Potential of AAV vectors in the treatment of metabolic disease. *Gene Ther.*, **15**, 831–839.

34. Seppen, J., Bakker, C., de Jong, B., Kunne, C., van den Oever, K., Vandenberghe, K., de Waart, R., Twisk, J. and Bosma, P. (2006) Adeno-associated virus vector serotypes mediate sustained correction of bilirubin UDP glucuronosyltransferase deficiency in rats. *Mol. Ther. J. Am. Soc. Gene Ther.*, **13**, 1085–1092.

35. Boutin, S., Monteilhet, V., Veron, P., Leborgne, C., Benveniste, O., Montus, M.F. and Masurier, C. (2010) Prevalence of Serum IgG and Neutralizing Factors Against Adeno-Associated Virus (AAV) Types 1, 2, 5, 6, 8, and 9 in the Healthy Population: Implications for Gene Therapy Using AAV Vectors. *Hum. Gene Ther.*, **21**, 704–712.

36. Park, F. and Kay, M.A. (2001) Modified HIV-1 based lentiviral vectors have an effect on viral transduction efficiency and gene expression in vitro and in vivo. *Mol. Ther. J. Am. Soc. Gene Ther.*, **4**, 164–173.

37. Grinshpun, A., Condiotti, R., Waddington, S.N., Peer, M., Zeig, E., Peretz, S., Simerzin, A., Chou, J., Pann, C.-J., Giladi, H., *et al.* (2010) Neonatal gene therapy of glycogen storage disease type Ia using a feline immunodeficiency virus-based vector. *Mol. Ther. J. Am. Soc. Gene Ther.*, **18**, 1592–1598.
38. Aguilera-Méndez, A., Álvarez-Delgado, C., Hernández-Godinez, D. and Fernandez-Mejia, C. (2013) Hepatic diseases related to triglyceride metabolism. *Mini Rev. Med. Chem.*, **13**, 1691–1699.
39. Duan, X.-Y., Zhang, L., Fan, J.-G. and Qiao, L. (2014) NAFLD leads to liver cancer: do we have sufficient evidence? *Cancer Lett.*, **345**, 230–234.
40. Petta, S. and Craxì, A. (2010) Hepatocellular carcinoma and non-alcoholic fatty liver disease: from a clinical to a molecular association. *Curr. Pharm. Des.*, **16**, 741–752.
41. Nair, N., Rincon, M.Y., Evens, H., Sarcar, S., Dastidar, S., Samara-Kuko, E., Ghandeharian, O., Man Viecelli, H., Thöny, B., De Bleser, P., *et al.* (2014) Computationally designed liver-specific transcriptional modules and hyperactive factor IX improve hepatic gene therapy. *Blood*, **123**, 3195–3199.
42. Chuah, M.K., Petrus, I., De Bleser, P., Le Guiner, C., Gernoux, G., Adjali, O., Nair, N., Willems, J., Evens, H., Rincon, M.Y., *et al.* (2014) Liver-specific transcriptional modules identified by genome-wide in silico analysis enable efficient gene therapy in mice and non-human primates. *Mol. Ther. J. Am. Soc. Gene Ther.*, **22**, 1605–1613.
43. Brown, B.D., Venneri, M.A., Zingale, A., Sergi, L. and Naldini, L. (2006) Endogenous microRNA regulation suppresses transgene expression in hematopoietic lineages and enables stable gene transfer. *Nat. Med.*, **12**, 585–591.
44. Bovia, F., Salmon, P., Matthes, T., Kvell, K., Nguyen, T.H., Werner-Favre, C., Barnet,

- M., Nagy, M., Leuba, F., Arrighi, J.-F., *et al.* (2003) Efficient transduction of primary human B lymphocytes and nondividing myeloma B cells with HIV-1-derived lentiviral vectors. *Blood*, **101**, 1727–1733.
45. Follenzi, A., Ailles, L.E., Bakovic, S., Geuna, M. and Naldini, L. (2000) Gene transfer by lentiviral vectors is limited by nuclear translocation and rescued by HIV-1 pol sequences. *Nat. Genet.*, **25**, 217–222.
46. Zennou, V., Petit, C., Guetard, D., Nerhbass, U., Montagnier, L. and Charneau, P. (2000) HIV-1 genome nuclear import is mediated by a central DNA flap. *Cell*, **101**, 173–185.
47. Zufferey, R., Donello, J.E., Trono, D. and Hope, T.J. (1999) Woodchuck hepatitis virus posttranscriptional regulatory element enhances expression of transgenes delivered by retroviral vectors. *J. Virol.*, **73**, 2886–2892.
48. Pfleiderer, G. (1974) Glycogen: determination with amyloglucosidase. In *Methods of Enzymatic Analysis*, Verlag-Chemie. Bergmeyer HU, Deerfield Beach, FL, US, Vol. 2, pp. 59–62.
49. Bligh, E.G. and Dyer, W.J. (1959) A rapid method of total lipid extraction and purification. *Can. J. Biochem. Physiol.*, **37**, 911–917.
50. Pillot, B., Soty, M., Gautier-Stein, A., Zitoun, C. and Mithieux, G. (2009) Protein feeding promotes redistribution of endogenous glucose production to the kidney and potentiates its suppression by insulin. *Endocrinology*, **150**, 616–624.
51. Rajas, F., Jourdan-Pineau, H., Stefanutti, A., Mrad, E.A., Iyenedjian, P.B. and Mithieux, G. (2007) Immunocytochemical localization of glucose 6-phosphatase and cytosolic phosphoenolpyruvate carboxykinase in gluconeogenic tissues reveals unsuspected metabolic zonation. *Histochem. Cell Biol.*, **127**, 555–565.

LEGENDS TO FIGURES

Fig. 1: Plasma parameter following during 9 months after lentiviral gene therapy.

(A) Blood glucose after 6h of fasting following during 9 months after gene deletion in WT (black squares), untreated L-G6pc^{-/-} (white squares), and HIV-G6PC treated L-G6pc^{-/-} mice (dark grey squares). Blood triglycerides (B) and total cholesterol (C) analysis after 6h of fasting at 1, 3, 6 and 9 months after tamoxifen treatment, in WT (black bars), untreated L-G6pc^{-/-} (white bars) and HIV-G6PC treated L-G6pc^{-/-} mice (dark grey bars). The results are expressed as the mean \pm SEM (n = 5 mice per group). The various groups were compared by one-way ANOVA followed by Tukey's post-hoc test. Values significantly different from WT mice (p<0.05*, p<0.01** and p<0.001***) and from untreated L-G6pc^{-/-} mice (p<0.05^{\$}, p<0.01^{\$\$} and p<0.001^{\$\$\$}) are indicated.

Fig. 2: Analysis of hepatic parameters after lentiviral gene therapy

(A) Liver weight compared to the body weight, (B) hepatic glucose-6-phosphate (G6P) content (C) hepatic glycogen content and (D) hepatic triglyceride content in WT (black bars), untreated L-G6pc^{-/-} (white bars), and HIV-G6PC treated L-G6pc^{-/-} mice (dark grey bars). Data were obtained at 9 months after *G6pc* deletion from mice fasted for 6h. The results are expressed as the mean \pm SEM (n = 5 mice per group). The various groups were compared by one-way ANOVA followed by Tukey's post-hoc test. Values significantly different from WT mice (p<0.01** and p<0.001***) and from untreated L-G6pc^{-/-} mice (p<0.05^{\$} and p<0.001^{\$\$\$}) are indicated.

Fig. 3: Histological analysis of the liver after lentiviral gene therapy

(A) H&E section staining from the WT (a), untreated L-G6pc^{-/-} (b), and HIV-G6PC treated L-G6pc^{-/-} mouse (c) livers. PP corresponds to the periportal area and PV to the perivenous region. (B) H&E staining (panel a) and immunohistochemical staining of G6PC (panel b) from serial sections of HIV-G6PC treated L-G6pc^{-/-} livers after 9 months of *G6pc* deletion. (C) Quantification of the human and mouse *G6pc* mRNA expression in the livers of untreated or HIV-G6PC treated WT or L-G6pc^{-/-} mice after 9 months of *G6pc* deletion. *G6pc* mRNA levels were expressed relatively to mL19 transcript. The asterisks correspond to undetectable value.

Fig. 4: Tumour development in L-G6pc^{-/-} mice

(A-B) Liver resection after 9 months of hepatic *G6pc* deletion. Arrows point nodules of about 3-4 mm of diameter. (C-F) Histological analysis by H&E staining of an HCA (C and E) and an HCC (D and F) developed in untreated L-G6pc^{-/-} mice. Panels E and F correspond to a higher magnification of the tumours observed in panels C and D, respectively.

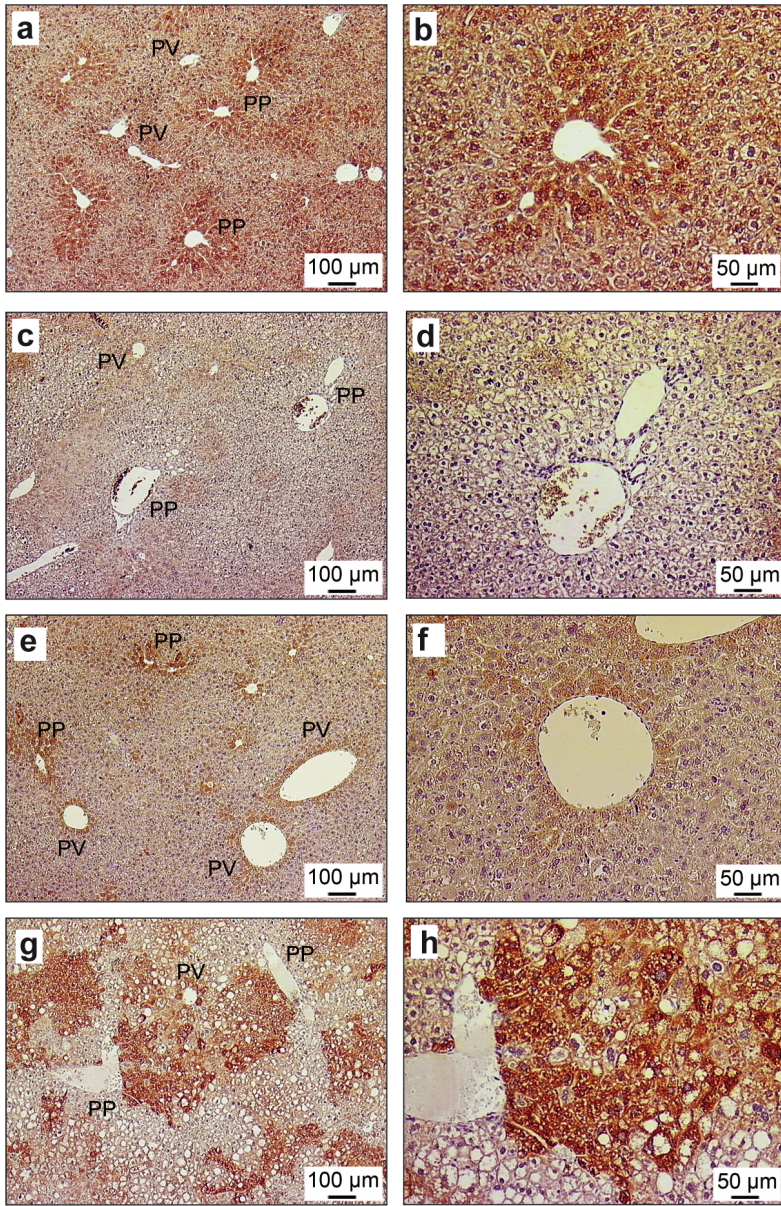
Fig. 5: HIV-G6PC vector transduction, dissemination and expression.

(A) Immunohistochemical analyses of G6PC in the liver of WT (a-b), untreated L-G6pc^{-/-} (c-d) and HIV-G6PC treated L-G6pc^{-/-} after 6 weeks (e-f) or 9 months of lentiviral transduction (g-h) mice. Panels b, d, f and h correspond to a higher magnification of the G6PC positive areas observed in panels a, c, e and g, respectively. PP corresponds to the periportal area and PV to the perivenous region. (B) Computerized quantification of G6PC positive hepatocytes detected by immunohistochemistry in the liver of HIV-G6PC treated mice at 6 weeks (dark grey bar) or 9 months (light grey bars) of lentiviral transduction. (C) G6Pase activity in the liver of WT (black bars), untreated L-G6pc^{-/-} (white bars) and HIV-G6PC treated mice at 9

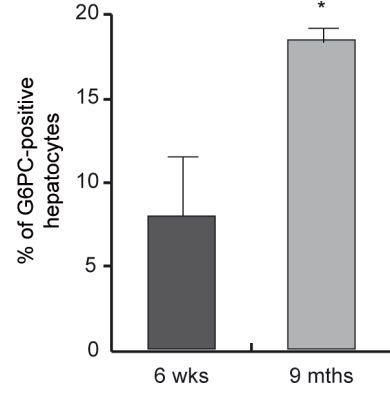
months of lentiviral transduction (light grey bars). (D) Determination of vector dissemination by PCR. Genomic DNA was extracted from various organs of HIV-G6PC treated L-G6pc^{-/-} mice. The presence of human G6PC cDNA was detected by PCR. As a control, a fragment from the murine *G6pc* gene was also amplified. The results are expressed as the mean \pm SEM (n = 5 mice per group). The various groups were compared by one-way ANOVA, followed by Tukey's post-hoc test for (B) and by an unpaired two-tailed Student's t-test (C). Values significantly different from WT mice (p<0.001***) and from untreated L-G6pc^{-/-} mice (p<0.001^{\$\$\$}) are indicated.

List of abbreviations: AAV, Adeno-associated virus; BM, Body Mass; G6P, glucose-6 phosphate; G6Pase, glucose-6 phosphatase; GSD1, glycogen storage disease type 1; HCA, hepatocellular adenoma; HCC, hepatocellular carcinoma; HIV, human immunodeficiency virus; mTTR, murine transthyretin; TG, triglycerides; WT, wild type.

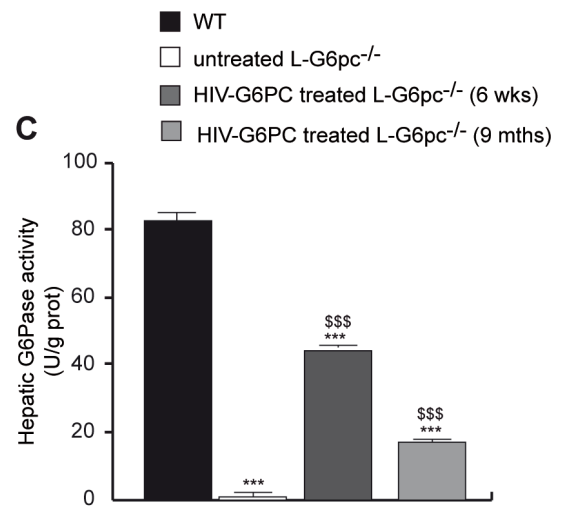
A



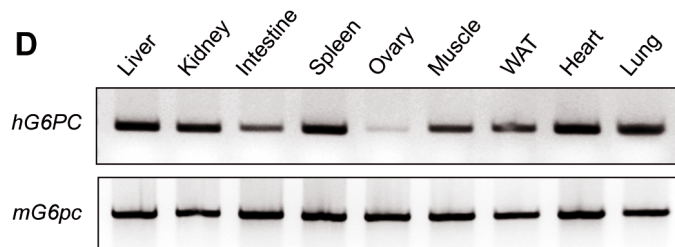
B

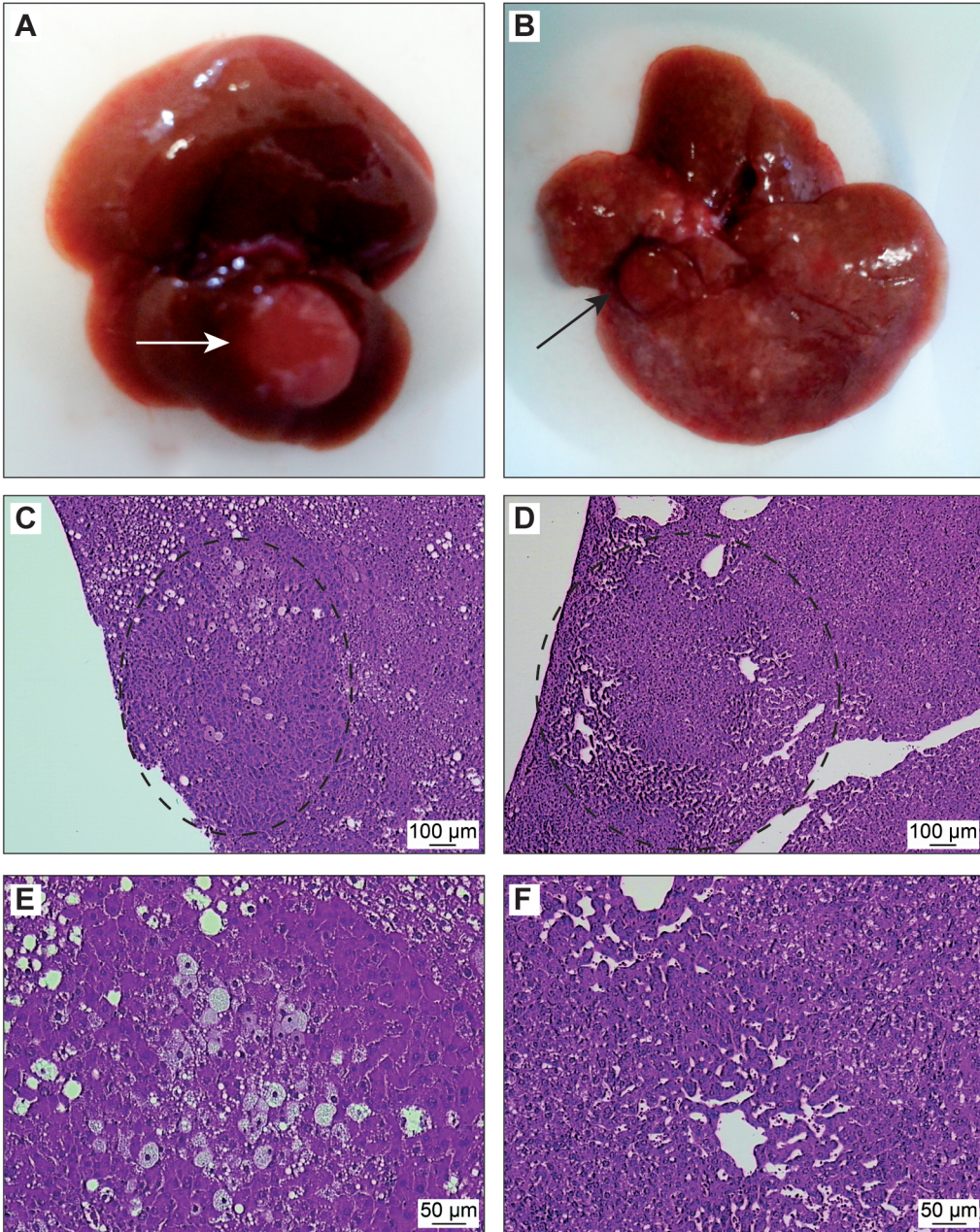


C



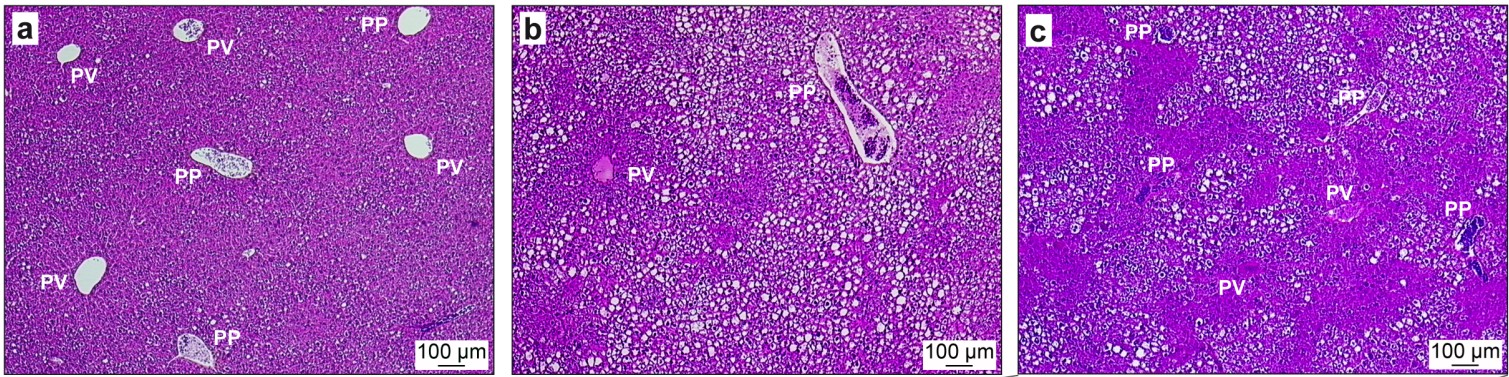
D



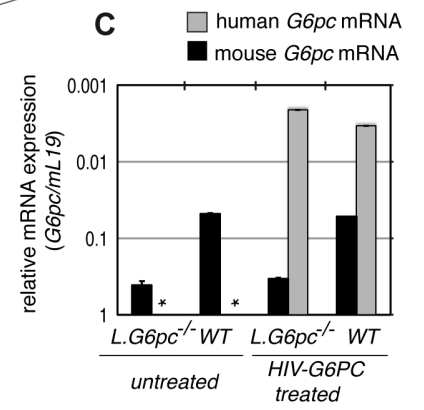
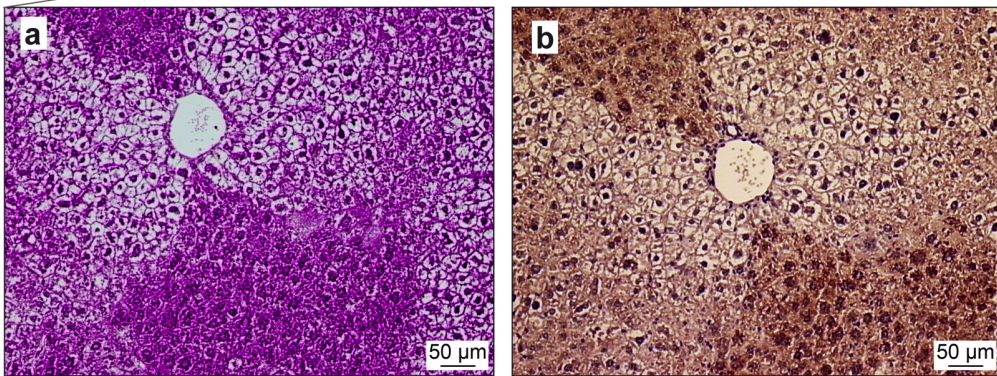


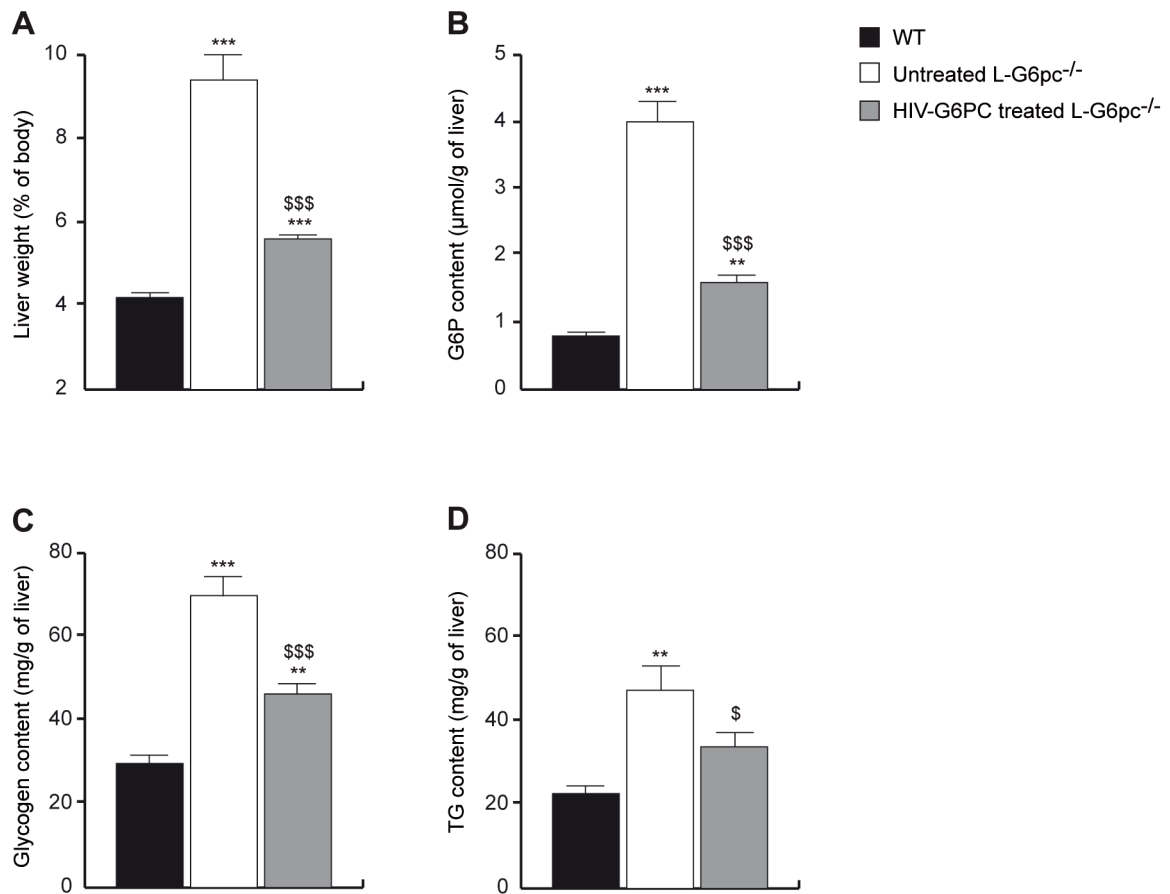
Clar et al., Figure 4

A

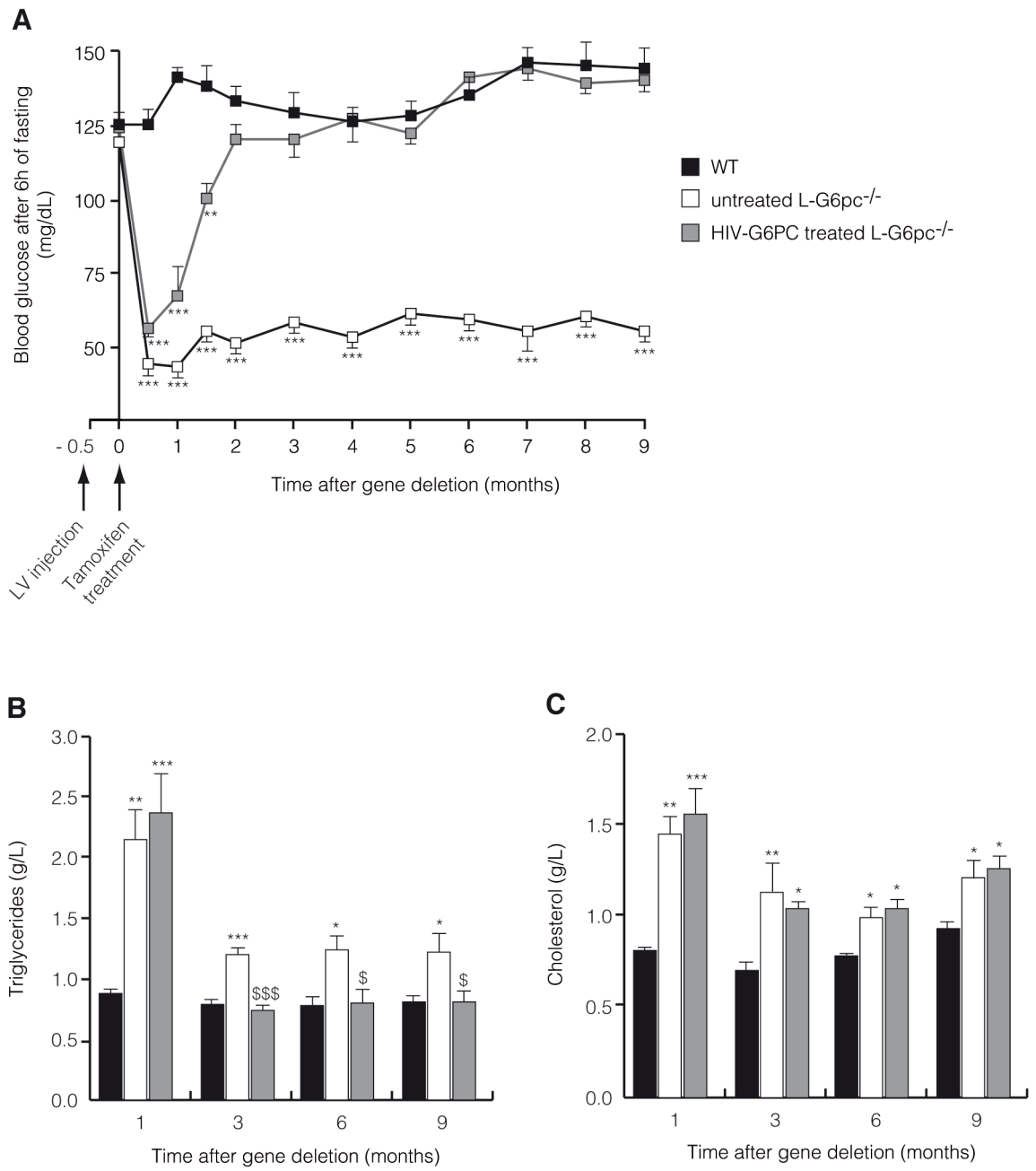


B





Clar et al., Figure 2



Clar et al., Figure 1